Infrared Spectroscopy of the Cyanide Complex of Iron(II) Myoglobin and Comparison with Complexes of Microperoxidase and Hemoglobin †

ARTICLE *in* BIOCHEMISTRY · MAY 1996

Impact Factor: 3.02 · DOI: 10.1021/bi952596m · Source: PubMed

7 AUTHORS, INCLUDING:

Solomon S Stavrov
Tel Aviv University
33 PUBLICATIONS **498** CITATIONS
SEE PROFILE

Jane M. Vanderkooi
University of Pennsylvania
144 PUBLICATIONS **4,938** CITATIONS
SEE PROFILE

Infrared Spectroscopy of the Cyanide Complex of Iron(II) Myoglobin and Comparison with Complexes of Microperoxidase and Hemoglobin†

K. S. Reddy,‡ T. Yonetani,‡ A. Tsuneshige,‡ B. Chance,‡ B. Kushkuley,§ S. S. Stavrov,§ and J. M. Vanderkooi*,‡

Johnson Research Foundation, Department of Biochemistry and Biophysics, School of Medicine, University of Pennsylvania, Philadelphia, Pennsylvania 19104, and Sackler Institute of Molecular Medicine, Sackler School of Medicine, Tel Aviv University, Tel Aviv 69978, Israel

Received November 1, 1995; Revised Manuscript Received January 23, 1996⊗

ABSTRACT: The cyanide complex of Fe^{II}Mb prepared and maintained at temperatures below 0 °C is sufficiently stable to permit spectroscopic characterization and allow comparison with free HCN and other ferric and ferrous CN complexes. The visible absorption spectrum of Fe^{II}Mb−CN has a split α band maxima at 571 and 563 nm, suggesting distortion in the x−y plane of the porphyrin. Fe^{II}Mb−CN, like the CO complex, was found to be optically active by circular dichroism. The C−N stretching frequencies for the CN−ferrous complexes are very sensitive to parameters within the heme pocket. The values are as follows: Fe^{II}Mb at pH 8, 2057 cm^{-1} with a shoulder appearing at 2078 cm^{-1} at pH 5.6; Fe^{II}Mp, 2034 cm^{-1}. In contrast, the frequencies for C−N stretch differ little among ferric heme complexes, ranging from 2123 to 2125 cm^{-1} for myoglobin, hemoglobin, and microperoxidase. These values compare with free HCN (2094 cm^{-1}) or CN^- (2080 cm^{-1}). Quantum chemical modeling of the neutral iron−porphyrin complex with imidazole and cyanide and of its anion was used to explain the effects of the cyanide coordination and of iron reduction on the C−N stretching frequencies. The lower νC−N for Fe^{II}Mb−CN relative to the ferric complex is attributed to the appearance of additional electron density on all the anti-bonding CN orbitals. The extra electron density was also used to explain that the band width of C−N stretching mode was greater in the ferrous complexes than in the ferric complex. Finally, the calculation shows that σ donation weakens the Fe−C bond, in qualitative agreement with the spontaneous dissociation of CN^- from Fe^{II}Mb at −5 °C. The sensitivity of CN complexes of ferrous heme proteins to the heme pocket environment and the ability to correlate spectroscopic parameters with calculated electron density suggest that infrared spectroscopy of the CN ligand is an appropriate tool to study ferrous heme proteins.

Many heme proteins share the same prosthetic group, heme IX, but differ in the axial coordination of the iron and the distal environment of the heme. In myoglobins (Mb's)[1] and hemoglobins (Hb's), the imidazole (Im) of histidine is one of the iron axial ligands, while the sixth coordination position is vacant or weakly ligated by the solvent. These heme proteins have the function to store and transport diatomics, requiring the coordination of diatomic molecules to the iron. In other heme proteins, the coordination of the diatomic molecule can lead to its activation through change of the interatomic distance, the force field constant, and the activation barrier of dissociation. For example, cytochrome P-450 breaks the O−O bond of coordinated dioxygen (Ullrich, 1979).

The nature of the proximal iron ligand, hydrogen bonds, steric and electrostatic interactions of the distal heme environment with the diatomic ligand, and the geometry of its coordination are essential factors through which the protein can regulate its storage, transport, or catalytic activities. One major problem is to discriminate between the different factors that affect heme protein function.

Infrared and resonance Raman vibrational spectroscopy allows one to "see" the bond directly, permitting the investigation of the effect of the proximal and distal heme environment on the activation of the diatomic ligand by heme proteins (Alben & Caughey, 1968; Caughey et al., 1969; Yoshikawa et al., 1985; Dong & Caughey, 1994). These methods applied to the CO complexes of hemes showed that even for Hb and Mb or for carbonylheme complex with neutral imidazole, the C−O stretching frequency, ν(CO), varies widely (from ∼1930 to 2015 cm^{-1}) (Babcock, 1988; Yu & Kerr, 1988; Ray et al., 1994). Several mechanisms were invoked to explain these variations. First, it was assumed that they can be caused by electron donor−acceptor interactions between the proximal nitrogen of the distal histidine and the coordinated CO. However, the distance between distal His and CO seems too large to allow the electron density transfer (Cameron et al., 1993; Quillin et al., 1993, 1995; Jewsbury & Kitagawa, 1994, 1995; Li et al., 1994). Second, distortion of the CO coordination geometry due to steric interaction with the distal environment

† This work was supported by National Institutes of Health Grant P01 GM 48130 and by the Sackler Fund for Scientists Absorption and the Center for Scientists Absorption (S.S.S.). The work done by B.K. is in partial fulfillment of the requirements for the Ph.D. degree from the Sackler School of Medicine at Tel Aviv University.

* To whom correspondence should be addressed. Phone: 215-898-8783. Fax: 215-573-2042. E-mail: vanderkooi@mscf.med.upenn.edu.

‡ University of Pennsylvania.

§ Tel Aviv University.

⊗ Abstract published in *Advance ACS Abstracts,* April 1, 1996.

[1] Abbreviations: IR, infrared; FT, Fourier transforms; CD, circular dichroism; Mb, myoglobin; Hb, hemoglobin; Mp, microperoxidase-11; FWHM, full width at half-maximum; MO, molecular orbital; Fe^{II}-P(Im)−CN, heme imidazole−CN complex; OEDT, orbital electron density transfer.

S0006-2960(95)02596-7 CCC: $12.00

was considered as another cause of the dependence of the FeCO properties on the protein structure. But, the latest results of X-ray diffraction studies of heme proteins (Springer et al., 1994) and data on model compounds (Ricard et al., 1986; Kim et al., 1989; Kim & Ibers, 1991) manifest the same linear perpendicular coordination of CO. The possibility of the Fe−C distance variation in different heme proteins and model compounds and the effect of this variation on the frequencies were discussed by Ray et al. (1994). Third, the effect of electrostatic interaction between the protein polar groups and the heme is now under intense scrutiny (Oldfield et al., 1991; Park et al., 1991; Li et al., 1994; Springer et al., 1994; Decatur & Boxer, 1995). The mechanism of this effect can be understood qualitatively: external electric field affects the orbital electron density transfer (OEDT) to and from the ligand bonding and anti-bonding orbitals. The electron density transfer changes the ligand force field constant and, consequently, the stretching frequency.

Quantum chemical calculations using OEDT and the vibronic theory of activation (Bersuker, 1978, 1984) allowed Stavrov and co-workers (Stavrov et al., 1993; Kushkuley & Stavrov, 1994) to quantitatively demonstrate that the main contribution to the CO properties by heme proteins stems from the electron density transfer from the iron to the 2π MO of the CO (π back-bonding), whereas the OEDT from the 5σ MO to Fe (σ donation) has a much weaker affect. Consequently, ν(CO) reflects mainly the effect of the protein electric field on the distribution of the π electrons of the FeCO unit. It was also shown that π donation and σ back-bonding depend on the protein electric field in different ways.

Other diatomics have varying contribution to π donation and σ back-bonding, and hence the protein field should have different influence on them. Cyanide represents an interesting comparison with CO because CN^- coordination to transition metal complexes is mainly affected by σ donation, π back-bonding being very weak (Cotton & Wilkinson, 1966; Nakomoto, 1978).

The CN complexes have one more advantage in that they complex with both the oxidized and reduced forms of iron (Keilin & Hartree, 1951, 1955). Cyanide binds to the ferric ion in heme proteins including metmyoglobin (Fe^{III}Mb) or methemoglobin (Fe^{III}Hb) with high affinity (Keilin & Hartree, 1955; McCoy & Caughey, 1970; Tang et al., 1994). Complexes of CN^- with ferrous heme proteins have been characterized for horseradish peroxidase (Rakshit & Spiro, 1974; Teroaka & Kitagawa, 1980; Yoshikawa et al., 1985; Meunier et al., 1995) and mixed-valence states of cytochrome oxidase (Caughey et al., 1993; Yoshikawa et al., 1995) while the complex with the ferrous form of myoglobin has only been reported for basic medium at high KCN concentrations (Balthazard & Phillipe, 1926; Keilin & Hartree, 1955) or observed transiently (Cox & Hollaway, 1977; Olivas et al., 1977; Bellelli et al., 1990). Since the ferrous system is electron-richer than the ferric, the protein electric field is expected to affect the electronic structure and properties of the reduced complex more than for the oxidized form.

In this paper, we define the conditions where the CN complex of iron(II) myoglobin (Fe^{II}Mb−CN) is sufficiently stable to characterize spectroscopically and examine the properties of the complex with the view of characterizing the environment of the heme pocket. We contrast the CN complex of myoglobin with that of microperoxidase-11(Mp). Mp is a fragment of cytochrome *c* with 11 amino acids and has the heme covalently bound to 2 cysteines. Because it is not a properly folded protein, the heme has a much more open site than Mb and interfaces with the solvent. The optical and infrared absorption spectra of the two complexes are interpreted using a quantum chemical approach.

EXPERIMENTAL PROCEDURES

Myoglobin from horse muscle type II from Sigma Chemical Co. (St. Louis, MO) was purified on a DEAE column using a pH gradient between 7 and 8 and 20 mM phosphate buffer. Microperoxidase from the same company was used without further purification. Symmetric mixed-valency hybrid hemoglobin (Hb) (i.e., α[Fe(III)−CN]$_2\beta$[Fe(II)−CO]$_2$ and α[Fe(II)−CO]$_2\beta$[Fe(III)−CN]$_2$) was prepared from human hemoglobin as previously described (Tsuneshige & Yonetani, 1994). The appropriate chains in the oxy form were oxidized with 1.1 equiv of $K_3Fe(CN)_6$ and then mixed with 1.5 equiv of KCN. After approximately 30 min of reaction at room temperature, the mixture was filtered through Sephadex G-25 fine (Sigma Chemical Co.) equilibrated with 10 mM sodium phosphate buffer, pH 7.4, to remove excess reagents. The complete conversion of the corresponding chains to the cyanmet form was checked by spectrophotometry. The derivative shows a broad peak at 540 nm. Subsequently, the cyanmet chains were mixed in an equimolar ratio with their complementary ones in the CO form and purified by ion-exchange chromatography using POROS 50 HS (PerSeptive Biosystems, Framingham, MA) with sodium phosphate buffer and a NaCl gradient.

To prepare the iron(II) heme−CN complexes, the Fe(III) complex was reduced by mixing in dithionite-buffered solution at temperatures below 0 °C. The dithionite solution was prepared by adding solid dithionite to buffer that had been deoxygenated by bubbling with Ar. The dithionite was 3−4 times molar excess to that of the heme; in addition to reducing Fe-heme−CN complex, it also effectively removes O_2 from the sample. For these experiments, we included 50% (v/v) ethylene glycol in the medium. Ethylene glycol prevented the sample from freezing, and unlike other cryosolvents is not viscous at the temperatures used, allowing for mixing of the sample. Furthermore, ethylene glycol is known not to disrupt the protein under these conditions (Douzou, 1977). The pH was adjusted using dilute HCl or NaOH and measured with a microelectrode suitable for small volumes (Microelectrodes Inc., Londonderry NH).

Optical spectroscopy was carried out with Hitachi 2000 and 3000 spectrometers with the cell compartment temperature regulated by a circulating water bath. For CD visible spectroscopy, an AVIV 62DS CD spectrometer equipped with a thermoelectric module was used to control the temperature. The sample optical density was <0.5 Au. A Bruker IFS 66 FTIR spectrometer equipped with a Globar source, a KBr splitter, and an MCT detector was used for the IR measurements. The sample holder had CaF_2 windows, and its path length was 0.05 mm for the IR measurements. The same instrument was used for high-resolution optical absorption measurements (Figure 6) except that a tungsten lamp and a quartz beam splitter were used. The temperature of the sample was controlled with a circulation bath from ambient temperature until −8 °C. For temperatures below that, a top-loading APD closed-cycle Helitran cryostat (Advanced Research Systems, Allentown, PA) was used. The

temperature was measured with a silicone diode near the sample. In this cryostat, the sample chamber is filled with He gas at atmospheric pressure, so that temperature variations between the sample and the sensing diode can be expected to be negligible. The cryostat window and sample holder windows were of sapphire.

The intermediate neglect of differential overlap (INDO) version of the MO−LCAO approach was used for quantum chemical calculation of the electronic structure of the ferro− and ferri−porphyrin complex with cyanide, Fe(P)(Im)(CN), simulating the active center of the proteins studied in the experimental part of this paper. This type of approach is based on the self-consistent solution of the Hartree−Fock equation with the inclusion of all the one-center exchange terms necessary for rotational invariance and accurate spectroscopic predictions, as well as an accurate description of integrals involving 3d atomic orbitals (Ridley & Zerner, 1973; Bacon & Zerner, 1979; Zerner et al., 1980; Anderson et al., 1986). In INDO, the one-center core integrals are obtained from just ionization potentials, and the ionization potentials and electronic affinities are used for calculations of the ground-state electronic configuration. The spin-restricted Hartree−Fock method was used for calculation using Mataga−Nishimoto parametrization (Ridley & Zerner, 1973; Bacon & Zerner, 1979; Zerner et al., 1980; Anderson et al., 1986). For quantum chemical calculations by this method, we used the ZINDO program, kindly supplied by Dr. M. Zerner, University of Florida. To calculate the OEDT's to and from CN, the MO's obtained by the INDO calculations were rewritten on the basis of the eigenfunctions of free CN and the atomic functions of other atoms. Then the occupations of the CN eigenfunctions in the complex were calculated as the Mulliken population of the corresponding orbitals.

For the calculations, the known structures of the porphyrin and imidazole rings (Eaton et al., 1978) were used. The distances Fe(III)−N_{Im} = 2.04 Å, Fe(III)−CN = 1.97 Å, and C−N = 1.17 Å were taken from X-ray studies of the heme proteins and the ferri−porphyrin complexes (Deatherage et al., 1976; Poulos et al., 1978; Scheidt et al., 1980), with Fe−C−N being linear and coordinated perpendicular to the heme plane.

RESULTS

Optical Spectra of Myoglobin and Microperoxidase. Addition of KCN to Fe^{III}Mb produces changes in the absorption spectrum, indicating the binding of CN^-. As shown in Figure 1, the Soret maximum of Fe^{III}Mb is at 409 nm, which shifts to 418 nm with KCN addition. The absorption of Fe^{III}Mb in the visible region shows two major bands at 505 and 635 nm [Figure 1 and see Antonini and Brunori (1971)]. The CN^- complex of Fe^{III} has an absorption band maximum at 543 nm. When Fe^{III}Mb−CN is reduced to Fe^{II}Mb−CN by dithionite at −5 °C in a 50% ethylene glycol solution, the Soret maximum is at 435.5 nm, and the major peak in the visible spectrum appears at 571 nm, with vibronic bands at 563, 542, 536, and 527 nm. The spectrum of Fe^{II}Mb−CN is distinct from the absorption spectrum of Fe^{II}Mb which has a single transition in the visible region with a maximum at 552 nm. The near-infrared region is also shown in Figure 1. Fe^{II}Mb−CN shows broad absorption in the 1000−1100 nm region.

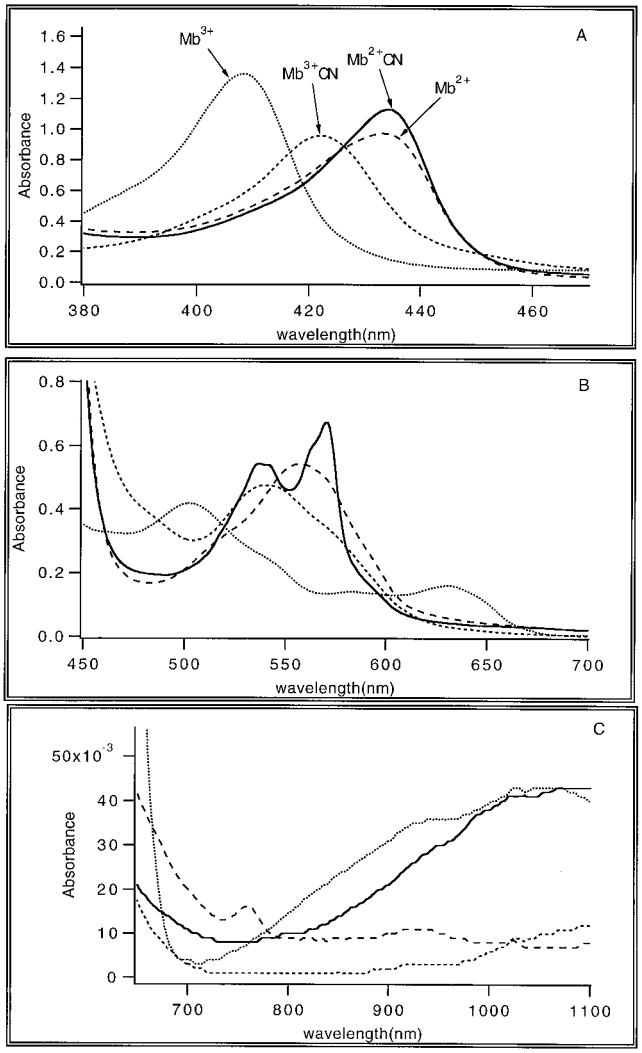

FIGURE 1: Optical spectra of Mb complexes. The dotted curve is Fe^{III}Mb; the short dash curve is Fe^{III}Mb−CN prepared by adding aliquots of a stock solution of 1 M KCN, pH 7.0, until no further change of the spectrum was observed (Tang et al., 1994). Solid curves, $Na_2S_2O_4$ added to Fe^{III}Mb−CN. Dashed curve, Fe^{II}Mb prepared by addition of $Na_2S_2O_4$ to Fe^{III}Mb. Temperature: −5 °C. Solvent was 50/50% (v/v) 100 mM potassium phosphate buffer, pH 7.0, and ethylene glycol. [Mb] was 10 μM (A) and 30 μM (B and C).

CN^- binds Mp in both its ferric and its ferrous forms. The Soret maxima for Fe^{III}Mp, Fe^{II}Mp, Fe^{III}Mp−CN, and Fe^{II}Mp−CN are at 401, 417, 411, and 419 nm, respectively (Figure 2). In the visible region, the major optical transition of Fe^{III}Mp is at 525 nm with a smaller transition at 622 nm. Addition of CN^- to Fe^{III}Mp yields a single visible band with a maximum at 530 nm, similar to Fe^{III}Mb−CN. Addition of dithionite to Fe^{III}Mp−CN gives band positions at 524 and 552.5 nm. Fe^{II}Mp has two optical bands at 522 and 550 nm (Figure 2). This is in contrast to Fe^{II}Mb where only a single broad band is seen (Figure 1).

As a further characterization of the CN^- complexes of the ferrous hemes, the visible CD spectra were taken (Figure 3). For both species, resolved CD spectra are obtained, with the α maximum shifted to the blue relative to the absorption spectra. The CD maximum wavelengths are at 565 and 551 nm for the Fe^{II}Mb and Fe^{II}Mp CN complexes, respectively. Unligated porphyrins and bis-ligated porphyrins are CD-inactive in the visible spectral region, and therefore CD supports the evidence that a CN complex is formed.

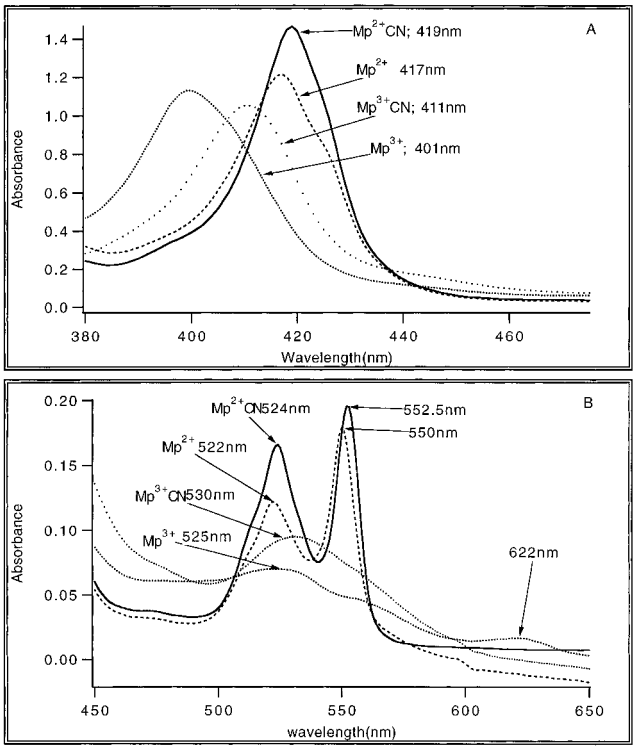

FIGURE 2: Optical spectra of Mp-11. The dotted curve is $Fe^{III}Mb$; the dotted-space curve is $Fe^{III}Mp-CN$ prepared by adding aliquots of a stock solution of 1 M KCN, pH 7.0, until no further change of the spectrum was observed; solid curve, $Na_2S_2O_4$ added to Fe^{III}-Mp−CN; dashed curve, $Fe^{II}Mp$ prepared by addition of $Na_2S_2O_4$ to $Fe^{III}Mp$. Temperature: 20 °C. Solvent was 100 mM potassium phosphate buffer, pH 7.0.

Kinetics of Cyanide Dissociation. The reduction of Fe^{III}-Mb−CN was achieved by adding dithionite as described under Experimental Procedures. Changes in the absorption spectrum of the prepared $Fe^{II}Mb-CN$ were then monitored as a function of time. Even at −5 °C, $Fe^{II}Mb-CN$ undergoes CN dissociation, and the spectrum changed into that of Fe^{II}-Mb over a period of several minutes (Figure 4). Clear isobestic points are seen at 428, 445, 517, 546, 560, and 577 nm, an indication that only two species are present. The reaction is thus consistent with a simple sequence: $Fe^{II}Mb-CN \rightarrow Fe^{II}Mb + CN^-$. The vibrational fine structure evident in both the α and β bands for $Fe^{II}Mb-CN$ is also clearly shown in Figure 4. The last spectrum of the figure is of deoxymyoglobin, consistent with the absence of O_2 in the sample.

The dissociation was followed at 571 nm as a function of time (Figure 5). The reaction is single-exponential as indicated by the correspondence of the experimental points with a calculated exponential function. The rate constant is 5.9×10^{-3} s^{-1} at pH 7.0 in 50% ethylene glycol and at −5 °C.

The isosbestic point in the absorption spectra following dissociation (Figure 4) and the exponential dissociation kinetics (Figure 5) suggest that a simple dissociation process occurs. However, subtleties are evident at lower temperature. In Figure 6, the absorption spectrum at high resolution of $Mb^{II}-CN$ at 100 K is shown. It is seen that the α band is definitely composed of two peaks and that there is vibrational fine structure in the higher energy region. Below 180 K, irradiation with the tungsten lamp produced no changes in the spectrum, but at around 200 K the sample was photolabile. The spectrum of the product of photoirradiation is distinct from $Fe^{II}Mb$ and $Fe^{II}MbCN$, indicating the presence of an intermediate in the dissociation reaction (Figure 6B). Warming this sample to 270 K gives the $Fe^{II}Mb$ spectrum shown in Figure 1 (Figure 6C), which shows that this intermediate ultimately yields $Fe^{II}Mb$.

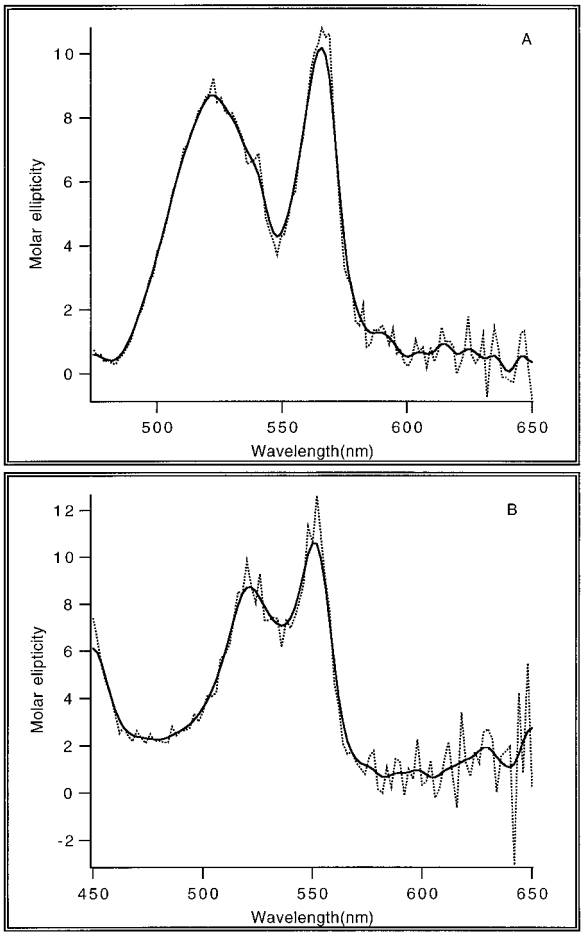

FIGURE 3: Circular dichroism spectra of $Mb^{II}CN$ (A) and $Mp^{II}CN$ (B) in the visible region. (A) −10 °C; solvent composition same as Figure 1. Spectral resolution at 0.5 nm. (B) 4 °C; solvent composition same as Figure 2. Spectral resolution at 1 nm. The light line is the original spectrum; the line is a fit curve using a smoothing routine.

In the case of $Fe^{II}Mb-CN$, no changes are seen in the time scale studied (hours) at −5 and 20 °C and pH 7, attesting that the complex is stable.

Infrared Spectra of CN in Heme Complexes. In Figure 7 the IR spectra of CN bound to ferric and ferrous iron in Mb and Mp are compared at two pHs. $Fe^{III}Mb-CN$ and Fe^{III}-Mp−CN gave frequencies that varied only by 2 cm^{-1}, i.e., 2126 and 2124 cm^{-1}, respectively. These values are independent of pH in the range of 6−8. The peak position of ν(CN) in Mp−CN is the same as that reported for Hb (McCoy & Caughey, 1970). Since there may be preferential binding of CN to one of the hemoglobin subunits, we also examined the frequency of CN bound to hemoglobin hybrids. CN bound to the α or β subunit as well as mixed hemoglobins like αCOβCN and αCNβCO gave stretching frequencies of 2123−2124 cm^{-1}, and these values were independent of whether CO was bound to the other subunit (spectra not shown).

Unlike the ferric complexes, the IR transitions of CN in ferrous Fe(II) heme complexes are sensitive to environment.

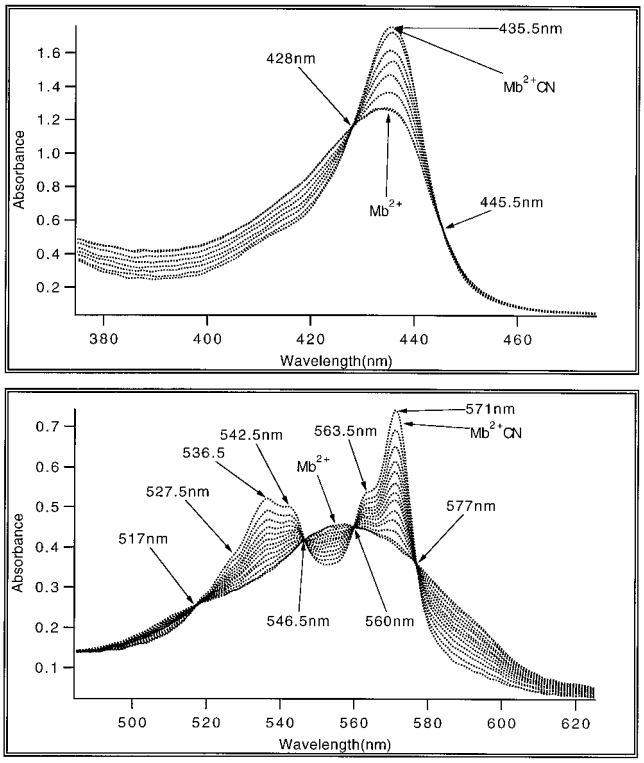

FIGURE 4: Spontaneous dissociation of $Mb^{II}CN$ to deoxyMb. Fe^{III}-Mb−CN was prepared as in Figure 1, and then reduced to Fe^{II}-Mb−CN by dithionite addition at −5 °C. The spectra were recorded at 100 s intervals after reduction. The curve, indicated by Mb^{2+}, is Fe^{II}Mb prepared by dithionite addition to Fe^{III}Mb. Solvent and temperature are the same as for Figure 1.

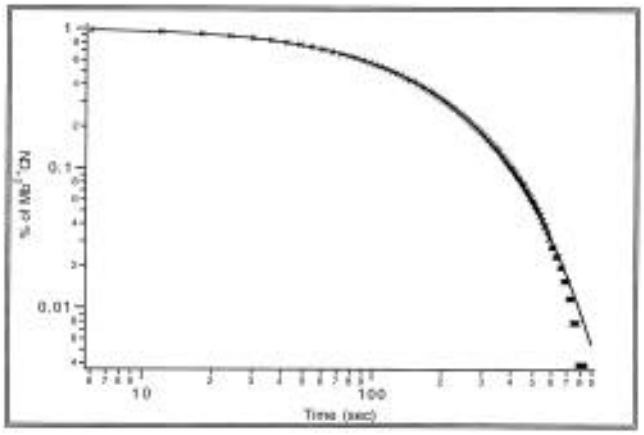

FIGURE 5: Kinetics of dissociation of Fe^{II}Mb−CN as a function of time at −5 °C. Absorption at 571 nm. Sample conditions given in Figure 4.

Reduction of Fe in Mb shifts the CN peak to lower frequency—2057 cm^{-1} at neutral pH and 2078 cm^{-1} at acidic pH (Figure 7B,D). This compares with 2034 cm^{-1} for Fe^{II}-Mp−CN. For both Mb and Mp, the CN stretching bands are broader and the extinction coefficients are higher for the ferrous−CN complex relative to the ferric form.

In the spectra shown in Figure 7, the peak at 2094 cm^{-1} is due to free CN^- (McCoy & Caughey, 1970). KCN in solution at pH 7 absorbs at 2094 cm^{-1}, the same frequency as CN in the KBr pellet (McCoy & Caughey, 1970). As the pH is raised, a new transition occurs at 2075−2080 cm^{-1}, concomitant with the disappearance of the absorption at 2094 cm^{-1} (not shown); the midpoint for this transition was at pH 9.3, consistent with the p*K* of HCN.

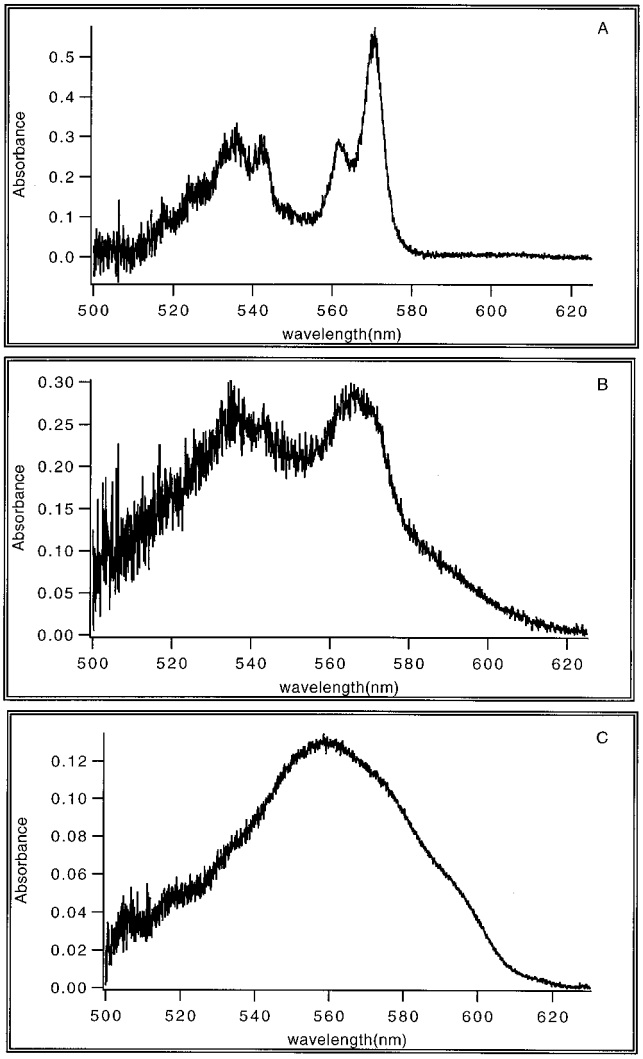

FIGURE 6: High-resolution absorption spectrum of Mb^{II}−CN. The sample was prepared at −20 °C and then mounted on the cell holder for the FTIR−Vis spectrophotometer. Path length was 50 μm. Temperature: (A) 100 K; (B) sample warmed to 200 K, allowing the measured light to irradiate the sample. The time of irradiation was about 10 min. (C) Sample further warmed during light irradiation to 270 K.

The CN stretching frequencies, band widths, and extinction coefficients for the compounds studied, and for horseradish peroxidase, are summarized in Table 1.

Calculation of Electronic Structure. The electronic structure of the neutral heme-imidazole−CN complex [Fe(P)-(Im)−CN] and of its anion was examined using the INDO quantum chemical calculations. The results of these calculations describing the effect of CN coordination and of the reduced complex on the atomic charges of the FeCN unit [*Q*(Fe), *Q*(C), and *Q*(N), respectively], C−N and Fe−C atomic bond indexes [*B*(C−N) and *B*(Fe−C), respectively], and the population of 4σ, 5σ, and 2π* molecular orbitals (MO) of CN [*q*(4σ), *q*(5σ), and *q*(2π*), respectively] are presented in Table 2.

DISCUSSION

Formation of Fe^{II}Mb−CN. The data presented here show that the CN complex of Fe^{II}Mb can be prepared in stable form by reducing Fe^{III}Mb−CN at low temperature. Evidence that the complex is formed is indicated by changes in the

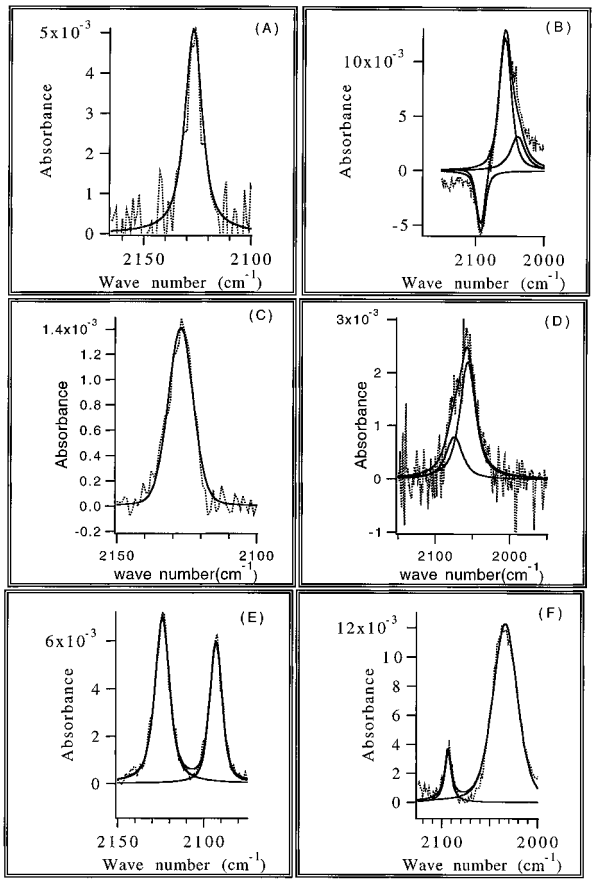

FIGURE 7: Infrared spectra of CN complexes of Mb and Mp. (A) Fe^{III}Mb−CN, pH 7.8; (B) Fe^{II}Mb−CN, pH 7.8; (C) Fe^{III}Mb−CN, pH 5.3; (D) Fe^{II}Mb−CN, pH 5.3; (E) Fe^{III}Mp−CN, pH 7.0; (F) Mp^{II}−CN, pH 7.0. The peak at 2094 cm^{-1} in panels E and F is that of free HCN. All spectra are the difference from the buffer spectrum except panel B, in which the reference is Fe^{III}Mb−CN. The inverted peak at 2094 cm^{-1} in panel B is also of free HCN and arose because the CN concentration was not exactly matched. The concentration of the heme protein was ∼8−10 mM; CN^- concentration was ∼10−15 mM.

visible and CD spectra as well as direct observation of the CN absorption in the infrared. The optical spectrum of the Fe^{II}Mb−CN complex is vibrationally resolved and particularly noticeable is a split in the α band (Figure 1 and Figure 4). Well-defined α and β bands are characteristic of complexes where the iron is in plane, and a split in the α band is indicative of asymmetry of the electric field in the x−y plane. The CN complex of the α and β chains of hemoglobin, in contrast, shows a relatively symmetric α band (Brunori et al., 1992), which resembles qualitatively the spectrum of Fe^{II}Mp−CN (Figure 3). A split in the α band for hydrazine-bound Fe^{II}Mb was observed by Keilin, who decided it was not due to two species, but an altered symmetry (Keilin, 1966). The similarity of the spectrum for hydrazine and CN complexes of Fe^{II}Mb suggests that the iron is in a similar coordination state.

Stability of Fe^{II}Mb−CN. At neutral pH, the predominant form of cyanide is HCN, and considering that small neutral molecules can diffuse through protein matrixes (Calhoun et al., 1988; Wright et al., 1992), it is expected that the protein does not pose a large barrier for the diffusion of HCN to the Fe(III) site, where it binds as CN^-, making a net internal charge of 0. Upon reduction of the iron within Mb−CN, the net internal charge becomes −1. With dissociation, CN^- is formed, and the presence of a charged group within the heme pocket possibly contributes to the instability of Fe^{II}-Mb−CN.

In fluid solution at −5 °C, the dissociation reaction of CN from the Fe^{II}Mb−CN complex is rigorously exponential in the time range of seconds to minutes (Figure 5). This effect was also seen with CO recombination in this temperature and intermediate time range (Murray et al., 1988). This exponential behavior is in contrast to the behavior seen for CO recombination at cryogenic temperature where nonexponentially is interpreted in terms of conformational substates that are manifested because kT is less than the barrier between the substates (Austin et al., 1973; Hong et al., 1991). The finding of exponentially in the dissociation of CN^- from ferrous myoglobin also contrasts with that reported for hemoglobin, where cooperative effects could be seen (Brunori et al., 1992). Since CN^- dissociation could be initiated by reducing the ferric complex with an externally added photoreductant or by rapid mixing with reductant, this reaction can be used as a kinetic probe to study the effect of the protein matrix fluctuations on the diffusion of a small charged ion. In detail, the CN^- diffusion should differ from CO which has a hydrophobic docking site (Jackson et al., 1994; Lim et al., 1995); instead, the diffusion of CN^- presumably would be affected by charged residues in the protein.

During the course of the study, we observed that Fe^{II}-MbCN is photosensitive at low temperatures (Figure 6). The spectrum of the photolyzed Mb^{II}−CN appears to retain the defined α and β bands, suggesting that Fe is in-plane but lacks the vibrational fine structure of Mb^{II}−CN. Perhaps the negatively charged species near the heme in the photolyzed sample exerts enough of a field on the heme to broaden vibrational fine structure and abolish the x, y asymmetry. Photolysis has also been observed by Keilin and Hartree (1955) for the Mb^{II}−CN complex at high pH in the presence of 1 M KCN, although in this case the Fe(II) is likely to be no longer ligated to the proximal histidine.

Infrared Spectroscopy of CN Complexes. In a study of metal−CN complexes, El-Sayed and Sheline (1958) concluded that ν(CN) values of metal cyano complexes are influenced by the electronegativity and oxidation state of the metal. The CN^- ion upon coordination to a metal acts as a σ-donor by donating electrons to the metal and as a π-acceptor by accepting electrons from the metal. The electron-donating process raises ν(CN) because electrons are removed from the 5σ orbital, which is weakly antibonding. On the other hand, π back-bonding would decrease the bond strength and the value of ν(CN) because the electrons enter into the antibonding $2\pi^*$ orbital (Nakomoto, 1978).

This general conclusion was checked using the semiempirical INDO quantum chemical calculations of Fe^{III}(P)(Im)−CN and its anion, $[Fe^{II}(P)(Im)-CN]^-$ (Table 2). In addition to the above-mentioned 5σ and $2\pi^*$ MO's, the calculations indicate that the 4σ orbital of CN^- is essential to the Fe−CN chemical bond. All these orbitals are the antibonding orbitals of CN; therefore, σ-donation (decrease of the population of both 4σ and 5σ MO's upon CN^- coordination) is expected to increase ν(CN), while π back-bonding decreases ν(CN).

We now examine how the experimental findings (Table 1) correlate with the calculations for the heme−CN complex

Table 1: ν(CN), Line Widths, and Extinction Coefficients

compound	conditions	frequency (cm^{-1})	width (cm^{-1}, FWHM)	extinction coefficient ($L\ mM^{-1}\ cm^{-1}$)	reference
CN^-, free	pH 12	2080.1	15.9		*a*, *b*
HCN, free	pH 7	2094.1	11.6	0.05	*a*
KCN	KBr pellet	2093.7			*b*
Fe^{III}−CN complexes					
Fe^{III}Mb−CN	pH 6−8.5	2125−2126	13.3	0.25	*c*
Fe^{III}Mp-11−CN	pH 7	2124.2	8.6		*c*
αFe^{III}Hb−CN	pH 6−8	2124			*a*
βFe^{III}Hb−CN	pH 6−8	2123			*c*
αFe^{III}Hb−CN*β*Hb−CO	pH 7	2123			*c*
αFe^{III}Hb−CN*β*Hb−CN	pH 7	2123			*c*
Fe^{II}−CN complexes					
Fe^{II}Mb−CN	pH 7−8	2057.1	∼21	2.65	*c*
Fe^{II}Mp-11−CN	pH 7	2034.0	22.2		*c*
Fe^{II}HRP−CN[d]		2029	36		*d*

[a] McCoy & Caughey (1970). [b] Nakomoto (1978). [c] This work. The extinction coefficients are expressed in terms of CN. All pHs at 7 ± 0.2, unless otherwise indicated. Concentrations were 1−10 mM. Temperature: 25 °C for all ferric complexes and free CN; −5 °C for Fe^{III}Mb. [d] HRP, horseradish peroxidase (Yoshikawa et al., 1985).

Table 2: Effect of Fe(P)(Im)(CN) Reduction on the Electronic Structure of the FeCN Unit[a]

	Q(Fe) (e^-)	Q(C) (e^-)	Q(N) (e^-)	$q(4\sigma)$ (e^-)	$q(5\sigma)$ (e^-)	$q(2\pi^*)$ (e^-)	B(C−N)	B(Fe−C)
free CN^-		−0.40	−0.60	2	2	0	2.86	
Fe^{III}(P)(Im)−CN	+0.33	−0.01	−0.40	1.84	1.47	0.05	2.88	0.88
$[Fe^{II}$(P)(Im)−CN$]^-$	−0.17	−0.05	−0.52	1.86	1.65	0.07	2.79	0.78

[a] *Q*, charge density; *q*, bond index; *B*, bond order.

of model porphyrin atomic bond index and electron density (Table 2).

(1) The Value of ν(CN) Is Higher in the Ferri Complexes (e.g., 2123−2126 cm⁻¹), than for Free CN⁻ (2080 cm⁻¹) or HCN (2094 cm⁻¹, Table 1). Quantitative information about the effect of the coordination on the strength of the C−N bond can be obtained from the study of the changes of bond order B(C−N) values: the increase in atomic bond index corresponds to the stronger interatomic bond. In the case of Fe^{III}(P)(Im)−CN, the coordination increases the B(C−N) value from 2.86 to 2.88, implying that the C−N bond in this complex is *stronger* than in free CN^-, consistent with the *higher* ν(CN) in the complex.

(2) The Value of ν(C−N) of the Cyanide Complexes of Fe^{III}Mb and Fe^{II}Mp−11 Is Lower than for Free CN⁻. In the calculation, the appearance of additional electron density on the 4σ, 5σ, and $2\pi^*$ antibonding CN orbitals upon reduction leads to weakening of the C−N bond [B(C−N) decreases from 2.88 to 2.79, Table 2]. Note, however, that the considerable decrease of B(Fe−C) implies that the reduction must lengthen the Fe−CN bond—this lengthening was not taken into account in our calculations. The increase in the C−N bond would decrease the overlap between the cyanide and iron orbitals, reducing the calculated σ-donation and π back-bonding. Taking this into account, we can conclude that the reduction of the complex is expected to weaken the C−N bond, the magnitude of this weakening being less than the calculated one. The weakening of the bond explains the experimentally observed downshift in frequency.

(3) Fe^{II}Mb−CN Is Much Less Stable than Fe^{III}Mb−CN. One-electron reduction of the Fe(III) complex leads to the appearance of additional electron density of 0.66 e^- on the FeCN unit, to the increase of the population of all the MO's contributing to the Fe−CN chemical bond, and, as a result, to the increase of back-bonding and decrease of σ-donation, the latter being much stronger (Table 2). Since the σ-donation mainly contributes to the Fe−CN bond, these changes weaken the Fe−C bond; this qualitative conclusion is in agreement with the results on B(C−N) in the ferri and ferro complexes, 0.88 and 0.78, respectively (Table 2). This theoretical result is in agreement with the much weaker Fe−C bond in Fe^{II}Mb−CN than in Fe^{III}Mb−CN. As noted above, however, the observed binding constant for CN will also be affected by factors within the protein polypeptide chain, including charge distributions.

(4) There Is Considerable Difference between ν(CN) in Different Ferro−Heme Complexes and Very Weak Variances in the Ferri−Heme Compounds (Table 1). Since CN in the Fe(II) compounds is more negative than for Fe(III), the electrostatic interaction with the polar environment must be stronger in the ferro compounds relative to the respective ferri complex. Therefore, a change of the environment is also expected to affect ν(CN) in the ferro compounds relatively more.

The greater sensitivity to environment due to increased negativity upon reduction can also explain why the CN band widths in the ferro compounds are systematically larger relative to the corresponding ferri complexes. The stronger interaction between CN and the imposed electric fields of the neighboring amino acids within the protein or the solvent in the case of Mp would serve to broaden the line.

(5) The Frequency ν(C−N) of Fe^{II}Mp−CN Is Lower than That of Fe^{II}Mb−CN (Table 1). The interaction of the cyanide−heme complexes with water differs from the interaction with the polypeptide chain of the heme pocket in that the water molecules are free to rotate in the external electric field and are more polar than the heme pocket amino acids. The negative CN attracts the positive sides of the water dipoles and repulses the negative sides. As a result, the oriented water molecules produce an electric field which attracts additional electron density to the coordinated CN,

causing a reduction of ν(CN). The polarization of water around CN^- explains the considerably lower value of ν(CN) in Fe^{II}Mp−CN than in Fe^{II}Mb−CN both in the presence and in the absence of the distal distidine in the heme pocket, 2034 cm^{-1} and 2057 and 2078 cm^{-1}, respectively (Table 1). In the ferri−heme compounds, water also affects ν(CN) more than the heme pocket amino acids, but the difference is much weaker than for the reduced complex because of the smaller charge of CN^-.

In this regard, we can comment on the CN^- complex of horseradish peroxidase (Yoshikawa et al., 1985). The lower values of ν(C−N) in the cyanide complex of this peroxidase (Table 1) can be caused by the more polar environment of the heme and, especially, by the additional electron density transfer to CN^- from the proximal histidine which, for the peroxidase, contains a deprotonated imidazole (La Mar et al., 1982).

Finally, we point out that the sensitivity of ν(CN) bound to Fe^{II}Mb to changes within the heme environment resembles the well-studied CO ligand. In spite of the large negative charge on CN, it behaves in many ways like CO when it is bound to iron(II) heme proteins. Both ligands have a lower frequency when bound to the iron(II) heme proteins relative to free, indicating that in both cases the bond order is lowered upon complexation. For instance, ν(CO) for gas or argon matrix is 2143 cm^{-1}, but is 1943 and 1945 cm^{-1} for sperm whale and horse heart myoglobin, respectively (Alben & Gaughey, 1968; Caughey et al., 1969), and the value for CO bound to microperoxidase is 1951−1955 cm^{-1} (Laberge et al., 1995). The sensitivity of ν(CO) to the heme environment has further been elegantly demonstrated for the CO complex, where the effect of the heme pocket has been studied by a series of mutants (Cameron et al., 1993). The value of 1944 cm^{-1} for the wild type goes to 1966 cm^{-1} when His64 is exchanged for Val, and the value for the double mutant H64V−V68T is upshifted to 1984 cm^{-1}.

pH Dependency of Mb^{II}−CN. A final experimental point to be discussed is that the value of ν(CN) in Mb^{II}−CN is pH-dependent (Figure 7). It was shown earlier (Tian et al., 1993) that in Mb(CO) protonation of the distal imidazole leads to its displacement out of the heme pocket. As a result, at low pH, ν(CO) is about 20 cm^{-1} higher than that at neutral pH and is very close to ν(CO) in the myoglobin mutants with substituted distal histidine (Quillin et al., 1993; Li et al., 1994). It was concluded on the basis of a study of mutants and model compounds that the reduction of ν(CO) at neutral pH is caused by the electrostatic interaction between the distal histidine and heme−CO complex, this conclusion being supported by our theoretical calculations (Kushkuley & Stavrov, 1995). A close situation is expected in Fe^{II}Mb−CN, where at neutral pH the distal histidine is located inside the pocket, attracting additional electron density to the antibonding orbitals of the coordinated CN^- and, consequently, reducing ν(CN). One can imagine that at low pH there is an equilibrium between this protein configuration and the configuration with the histidine cation located out of the heme pocket and exposed to water. As in the case of Mb−CO, the histidine displacement is expected to increase ν(CN) in Fe^{II}Mb−CN, leading to the appearance of the high-frequency shoulder (Table 1). The appearance of the shoulder at pH 5.6 implies that the p*K* of the distal histidine is close to this value, being considerably lower than that of the free histidine. This lowering of the distal histidine p*K* can be caused by the electrostatic interaction with the amino acids forming the heme pocket and with the heme−CN complex itself. Such an electron density redistribution has to make N_δ more positive, and, consequently, has to decrease the energy of the bond between this nitrogen and proton. As a result, a decrease of the CN charge is expected to decrease the p*K* of the distal histidine.

This conclusion is consistent with the absence of the high-frequency shoulder in Fe^{III}Mb−CN at pH 6, because in the oxidized state there is decreased charge of the whole iron(III) heme−CN unit (see Table 2) and, as mentioned in the previous paragraph, this decreases the p*K* of the distal histidine to a value lower than that in Fe^{II}Mb−CN. As a result, in ferrimyoglobin, the p*K* of the distal histidine is lower than 5.6, its cation is not formed in the studied pH range, and only one value of ν(CN) (2126 cm^{-1}) is observed which corresponds to the configuration with the distal histidine located inside the pocket.

Summary. Cyanide complexes of the ferro-heme proteins and their models were prepared in aqueous solutions and studied using optical and infrared spectroscopies. Combined application of FTIR spectroscopy and quantum chemical calculations of ferro− and the ferri−cyanide complexes allowed characterization of the complex. It was shown that in Fe^{II}-P(Im)−CN, relative to the ferri complex, there is increased electron density on the coordinated CN and, in particular, population of the CN anti-bonding orbitals. These results explain the red shift of the C−N infrared absorption band and its broadening in Mb−CN and Mp−CN, and the lower stability of the ferrous−CN complex. Since vibrational spectral features of the Fe−CN complexes are sensitive to the protein environment in a way that can be understood by the quantum chemical calculations, it is suggested that CN ligation can be used as a tool to monitor the environment of the heme pocket within heme proteins.

REFERENCES

Alben, J. O., & Caughey, W. S. (1968) *Biochemistry 7*, 175−183.
Anderson, W. P., Edwards, W. D., & Zerner, M. C. (1986) *Inorg. Chem. 25*, 2728−2732.
Antonini, E., & Brunori, M. (1971) in *Hemoglobin and Myoglobin in their Reactions with Ligands*, North-Holland, Amsterdam.
Austin, R. H., Beeson, K., Eisenstein, L., Frauenfelder, H., Gunsalus, I. C., & Marshall, V. P. (1973) *Science 181*, 541−543.
Babcock, G. T. (1988) in *Biological Applications of Raman Spectroscopy* (Spiro, T. G., Ed.) pp 292−346, Wiley-Interscience, New York.
Bacon, A. D., & Zerner, M. C. (1979) *Theor. Chim. Acta 53*, 21−54.
Balthazard, V., & Phillipe, M. (1926) *Ann. Med. Leg. Criminol. Police Sci. 6*, 137−143.
Bellelli, A., Antonini, G., Brunori, M., Springer, B. A., & Sligar, S. G. (1990) *J. Biol. Chem. 265*, 18898−18901.
Bersuker, I. B. (1984) *The Jahn-Teller Effect and Vibronic Interactions in Modern Chemistry*, Plenum, New York.
Brunori, M., Antonini, G., Castagnola, M., & Bellelli, A. (1992) *J. Biol. Chem. 267*, 2258−2263.
Calhoun, D. B.; Englander, S. W., Wright, W. W., & Vanderkooi, J. M. (1988) *Biochemistry 27*, 8466−8474.
Cameron, A. D., Smerdon, S. J., Wilkinson, A. J., Habash, J., Helliwell, J. R., Li, T. S., & Olson, J. S. (1993) *Biochemistry 32*, 13061−13079.
Caughey, W. S., Alben, J. O., McCoy, S., Charache, S., Hathway, P., & Boyer, S. (1969) *Biochemistry 8*, 59−62.
Caughey, W. S., Dong, A., Sampath, V., Yoshikawa, S., & Zhao, X.-J. (1993) *J. Bioenerg. Biomembr. 25*, 81−91.

Cotton, F. A., & Wilkinson, G. (1966) *Advanced Inorganic Chemistry. A Comprehensive Text*, Interscience Publishers/John Wiley & Sons, New York.
Cox, R. P., & Hollaway, M. R. (1977) *Eur. J. Biochem. 74*, 575−587.
Deatherage, J. F., Loe, R. S., Anderson, C. M., & Moffat, K. (1976) *J. Mol. Biol. 104*, 687−706.
Decatur, S. M., & Boxer, S. G. (1995) *Biochem. Biophys. Res. Commun. 212*, 159−164.
Dong, A., & Caughey, W. S. (1994) *Methods Enzymol. 232*, 139−175.
Douzou, P. (1977) *Cryobiochemistry. An Introduction*, Academic Press, London.
Eaton, W. A., Hanson, L. K., Stephens, P. J., Sutherland, J. C., & Dunn, B. V. R. (1978) *J. Am. Chem. Soc. 100*, 4991−5003.
El-Sayed, M F., & Sheline, R. K. (1958) *J. Inorg. Nucl. Chem. 6*, 187−193.
Hong, M. K., Shyamsunder, E., Austin, R. H., Gerstman, B. S., & Chan, S. S. (1991) *Biophys. J. 57*, 369−373.
Jackson, P., & Kitagawa, T. (1994) *Biophys. J. 67*, 2236−2250.
Jewsbury, P., & Kitagawa, T. (1994) *Biophys. J. 67*, 2236−2250.
Jewsbury, P., & Kitagawa, T. (1995) *Biphys. J. 68*, 1283−1294.
Keilin, J. (1966) in *Hemes and Hemoproteins* (Chance, B., Estabrook, R. W., & Yonetani, T., Ed.) pp 173−191, Academic Press, New York.
Keilin, D., & Hartree, E. F. (1951) *Biochem. J. 49*, 88−94.
Keilin, D., & Hartree, E. F. (1955) *J. Biochem. 81*, 495−503.
Kim, K., & Ibers, J. A. (1991) *J. Am. Chem. Soc. 113*, 6077−6081.
Kim, K., Fettinger, J., Sessler, J. L., Cyr, M., Hugdahl, J., Collman, J. P., & Ibers, J. A. (1989) *J. Am. Chem. Soc. 111*, 403−405.
Kushkuley, B., & Stavrov, S. S. (1994) *Abstracts of EUROBIC II: Metal in Biological Systems*, p 202.
Kushkuley, B., & Stavrov, S. S. (1996) *Biophys. J. 70*, 1214−1229.
Laberge, M., Vanderkooi, J. M., & Wright, W. (1995) *Photochem. Photobiol. 61*, A225.
La Mar, G. N., De Ropp, J. S., Chacko, V. P., Satterlee, J. D., & Erman, J. E. (1982) *Biochim. Biophys. Acta 708*, 317−325.
Li, T., Quillin, M. L., Phillips, G. N. J., & Olson, J. S. (1994) *Biochemistry 33*, 1433−1446.
Lim, M., Jackson, J. A., & Anfinrud, P. A. (1995) *Science 269*, 962−966.
McCoy, S., & Caughey, W. S. (1970) *Biochemistry 9*, 2387−2393.
Meunier, B., Rodiguez-Lopez, Smith, A. T., Thoerneley, R. N. F., & Rich, P. P. (1995) *Biochemistry 34*, 14687−14692.
Murray, L. P., Hofrichter, J., Henry, E. R., & Eaton, W. A. (1988) *Biophys. Chem. 29*, 63−76.
Nakomoto, K. (1978) *Infrared and Raman Spectra of Inorganic and Coordination Compounds*, John Wiley & Sons, New York.
Oldfield, E., Guo, K., Augspurger, J. D., & Dykstra, C. E. (1991) *J. Am. Chem. Soc. 113*, 7537−7541.
Olivas, E., de Waal, D. J. A., & Wilkins, R. G. (1977) *J. Biol. Chem. 252*, 4038−4042.
Park, K. D., Guo, K., Adebodun, F., Chiu, M. L., Sligar, S. G., & Oldfield, E. (1991) *Biochemistry 30*, 2333−2347.
Poulos, T. L., Freer, S. T., Alden, R. A., Xuong, N. H., Edwards, S. L., Hamlin, R. C., & Graut, J. (1978) *J. Biol. Chem. 253*, 3730−3735.
Quillin, M. L., Arduini, R. M., Olson, J. S., & Phillips, G. N., Jr. (1993) *J. Mol. Biol. 234*, 140−155.
Quillin, M. L., Li, T., Olson, J. S., Phillips, G. N., Jr., Dou, Y., Ikeda-Saito, M., Regan, R., Carlson, M., Gibson, Q. H., Li, H., & Elber, R. (1995) *J. Mol. Biol. 245*, 416−436.
Rakshit, G., & Spiro, T. G. (1974) *Biochemistry 13*, 5317−5323.
Ray, G. B., Li, X.-Y., Ibers, J. A., Sessler, J. L., & Spiro, T. G. (1994) *J. Am. Chem. Soc. 116*, 162−176.
Ricard, L., Weiss, R., & Momenteau, M. (1986) *J. Chem. Soc., Chem. Commun.*, 818−820.
Ridley, J., & Zerner, M. (1973) *Theor. Chim. Acta 32*, 111−134.
Scheidt, W. R., Haller, K. J., & Hatano, K. (1980) *J. Am. Chem. Soc. 102*, 3017−3021.
Springer, B. S., Sligar, S. G., Olson, J. S., & Phillips, G. N., Jr. (1994) *Chem. Rev. 94*, 699−714.
Stavrov, S. S., Decusar, I. P., & Bersuker, I. B. (1993) *New J. Chem. 17*, 71−76.
Tang, H.-L., Chance, B., Mauk, A. G., Powers, L. S., Reddy, K. S., & Smith, M. (1994) *Biochim. Biophys. Acta 1206*, 90−96.
Teroaka, J., & Kitagawa, T. (1980) *Biochem. Biophys. Res. Common. 93*, 694−700.
Tian, W. D., Sage, J. T., & Champion, P. M. (1993) *J. Mol. Biol. 233*, 155−166.
Tsuneshige, A., & Yonetani, T. (1994) *Methods Enzymol. 231*, 215−222.
Ullrich, V. (1979) *Top. Curr. Chem. 83*, 67−104.
Wright, W. W., Owen, C. S., & Vanderkooi, J. M. (1992) *Biochemistry 31*, 6539−6544.
Yoshikawa, S., O'Keeffe, D. H., & Caughey, W. S. (1985) *J. Biol. Chem. 260*, 3518−3528.
Yoshikawa, S., Mochizuki, M., Zhao, X.-J., & Caughey, W. S. (1995) *J. Biol. Chem. 270*, 4270−4279.
Yu, N. T., & Kerr, E. A. (1988) in *Biological Applications of Raman Spectroscopy* (Spiro, T. G., Ed.) pp 39−95, Wiley-Interscience, New York.
Zerner, M. C., Loew, G. H., Kirchner, R. E., & Mueller-Westerhoff, U. T. (1980) *J. Am. Chem. Soc. 102*, 589−599.

BI952596M